

Detection of an Electron Paramagnetic Resonance Signal in the S_0 State of the Manganese Complex of Photosystem II from *Synechococcus elongatus*[†]

Alain Boussac,*[‡] Helena Kuhl,[§] Elena Ghibaudi,[‡] Matthias Rögner,[§] and A. William Rutherford[‡]

Section de Bioénergétique, URA CNRS 2096, Département de Biologie Cellulaire et Moléculaire, CEA Saclay, 91191 Gif-sur-Yvette Cedex, France, and Lehrstuhl fuer Biochemie der Pflanzen, Fakultät fuer Biologie, Ruhr-Universität Bochum, Universitätsstrasse 150, 44780 Bochum, Germany

Received April 12, 1999; Revised Manuscript Received June 7, 1999

ABSTRACT: The Mn₄-cluster of photosystem II (PSII) from *Synechococcus elongatus* was studied by electron paramagnetic resonance (EPR) spectroscopy after a series of saturating laser flashes given in the presence of either methanol or ethanol. Results were compared to those obtained in similar experiments done on PSII isolated from plants. The flash-dependent changes in amplitude of the EPR multiline signals were virtually identical in all samples. In agreement with earlier work [Messinger, J., Nugent, J. H. A., and Evans, M. C. W. (1997) *Biochemistry* 36, 11055–11060; Åhring, K. A., Peterson, S., and Styring, S. (1997) *Biochemistry* 36, 13148–13152], detection of an EPR multiline signal from the S_0 state in PSII from plants was only possible with methanol present. In PSII from *S. elongatus*, it is shown that the S_0 state exhibits an EPR multiline signal in the absence of methanol (however, ethanol was present as a solvent for the artificial electron acceptor). The hyperfine lines are better resolved when methanol is present. The S_0 multiline signals detected in plant PSII and in *S. elongatus* were similar but not identical. Unlike the situation seen in plant PSII, the S_2 state in *S. elongatus* is not affected by the addition of methanol in that (i) the S_2 multiline EPR signal is not modified by methanol and (ii) the spin state of the S_2 state is affected by infrared light when methanol is present. It is also shown that the magnetic relaxation properties of an oxidized low-spin heme, attributed to cytochrome *c*₅₅₀, vary with the S states. This heme then is in the magnetic environment of the Mn₄ cluster.

Photosystem II (PSII)¹ catalyzes light-driven water oxidation resulting in oxygen evolution. The reaction center of PSII is made up of two membrane-spanning polypeptides (D1 and D2) analogous to the L and M subunits of the purple photosynthetic bacterial reaction center (see ref 1 for a review). Absorption of a photon results in a charge separation between a chlorophyll molecule (P₆₈₀) and a pheophytin molecule. The pheophytin anion transfers the electron to a quinone Q_A and P₆₈₀⁺ is reduced by a tyrosine residue, Tyr_Z. A cluster constituted of four manganese ions (Mn₄), located in the reaction center of PSII, probably acts both as the active site and as a charge-accumulating device of the water-splitting enzyme. During the enzyme cycle, the oxidizing

side of PSII goes through five different redox states that are denoted S_n, n varying from 0 to 4. Oxygen is released during the S₃ to S₀ transition in which S₄ is a transient state (2–6).

The structure of the Mn₄ cluster and the mechanism by which water is oxidized are still largely unknown. Currently, the most commonly discussed structure favored by extended X-ray absorption fine structure (EXAFS) experiments consists of a Mn tetramer which includes two di- μ -oxo(Mn₂) motifs (reviewed in ref 6). A multiline EPR signal has been detected near $g = 2$ in the S_2 state (7). This signal is spread over roughly 1800 G, is made up of at least 18 lines, each separated by approximately 80 G, and very probably arises from a magnetic tetramer that includes a di- μ -oxo(Mn^{III}Mn^{IV}) motif (7–9). The S_2 state can be quantitatively formed either by flash illumination in nonfrozen samples (7) or by continuous illumination at 200 K (8). Similar S_2 multiline signals have been detected in PSII isolated from plants (2–9), from the cyanobacteria, *Synechococcus* (11, 12) and *Synechocystis* (13–15), and from the green alga *Scenedesmus obliquus* (16, 17).

Under some experimental conditions (in the presence of sucrose in the buffer) the S_2 state gives rise to a $g = 4.1$ signal rather than a multiline signal (10, 18). The relative proportion of the multiline and $g = 4.1$ signals is affected by many biochemical treatments including the removal or the exchange of Ca²⁺ (2–6) and Cl[–] (2–6, 19–21), two essential cofactors for O₂ evolution. The $g = 4.1$ state can also be formed preferentially by illumination below 200 K

[†] This work was supported in part by grants from the Deutsche Forschungsgemeinschaft, SFB 480 (M.R. and H.K., H.K. by Graduiertenkolleg) and from the TMR program of the EC (Grants FMRX-CT96-0031 and FMRX-CT98-0214). E.G. was supported by a Marie Curie Fellowship from the TMR program of the European Community.

* To whom correspondence should be addressed: Fax 33 (0)1 69 08 87 17; Phone 33 (0)1 69 08 72 06; E-mail boussac@dsvidf.cea.fr.

[‡] CEA Saclay.

[§] Ruhr-Universität Bochum.

¹ Abbreviations: P₆₈₀, photooxidizable chlorophyll of photosystem II; PSII, photosystem II; Chl, chlorophyll; Tyr_Z, the tyrosine acting as the electron donor to P₆₈₀; Q_A, primary quinone electron acceptor of photosystem II; CW, continuous wave; cyt, cytochrome; EPR, electron paramagnetic resonance; PPBQ, phenyl-*p*-benzoquinone; MES, 2-(*N*-morpholino)ethanesulfonic acid; EDTA, ethylenediaminetetraacetic acid; IR, infrared; ESEEM, electron spin-echo envelope modulation; DCMU, 3-(3,4-dichlorophenyl)-1,1-dimethylurea; DMSO, dimethyl sulfoxide.

(10) if the light used is not free of infrared radiation (22). Absorption of radiation at ≈ 820 nm by the Mn_4 cluster induces a transition between a $S = 1/2$ state into a $S = 5/2$ state irrespective, at least below 200 K, of the temperature at which the sample is illuminated (22–25). At temperatures equal to or lower than 77 K, a state responsible for EPR signals with g values > 5 is trapped. Between 77 and 150 K, an activation barrier can be overcome and the next stable state becomes that responsible for the $g = 4.1$ signal (24). At temperatures higher than 150 K, the stable state is that responsible for the multiline signal (24).

A multiline EPR signal has also been observed in the S_0 state of PSII from plants (26–28). The detection in plant PSII of an S_0 signal by CW-EPR required the presence of methanol in the sample. The first observation of an EPR signal originating from the S_0 state (26) was done by two different methods to generate this state: (i) a chemical reduction with hydrazine of S_1 to S_{-1} followed by photo-generation of S_0 at 273 K in the presence of DCMU, and (ii) a chemical reduction with hydroxylamine of S_1 to S_0 . An S_0 EPR signal with an improved signal-to-noise ratio was obtained when this state was formed by illuminating dark-adapted samples (i.e., samples in the S_1 state) by three flashes with a Xe flash lamp (27) or by three laser flashes (28). The S_0 multiline signal, centered at $g = 2$, was spread over about 2000 G and has been proposed to originate from a Mn_4 cluster containing a di- μ -oxo($\text{Mn}^{\text{II}}\text{Mn}^{\text{III}}$) dimer (26–28). A temperature dependence study of the S_0 multiline signal has shown that the $S = 1/2$ state responsible for the signal is an isolated ground state (29).

Because PSII from thermophilic *Synechococcus* species is more stable than PSII either from plants or from *Synechocystis*, it has become a material widely used in attempts to generate single crystals (see, e.g., refs 30 and 31) for structural investigations by X-ray diffraction. It is therefore important to spectroscopically characterize in detail this kind of material and to compare it with PSII from plants.

Although previous EPR studies have shown that the S_2 EPR multiline signal in PSII from *S. elongatus* exhibits no significant differences compared to that in PSII from plants (see above), other methods have shown that differences between these two types of PSII do exist. For example, the S_2 and S_3 states are more stable, in intact cells, in *S. elongatus* than in plants (32); the temperature dependence of the $S_i \rightarrow S_{i+1}$ transition is also upshifted (33); and furthermore, the oxygen-evolving complex also shows unusual characteristics in studies of the effect of removal and reconstitution of anions and cations (e.g., 34, 35). In addition, the high-spin states, in S_2 , of PSII from *S. elongatus* slightly differed from those induced in PSII from plants. The value of the E/D ratio for the IR-induced state found in PSII isolated from *S. elongatus* was found to be more rhombic than that in PSII from plants and the $g = 4.1$ signal cannot be trapped in *S. elongatus* (25).

In the present study we report the detection of an S_0 EPR signal in PSII isolated from *S. elongatus* and a comparison with that observed in PSII isolated from spinach. The S states were generated by laser flash illumination. A comparison of the effect of methanol on the S_2 state in the two types of PSII preparations is also reported.

MATERIALS AND METHODS

PSII isolated from spinach were prepared as already described (22). Dimeric PSII from *S. elongatus* was extracted as in ref 36 except that 1.2% dodecyl β -maltoside instead of 1% was used. Further purification was done according to ref 37. Oxygen evolution activity of the PSII isolated from *S. elongatus* was about 5000 μmol of $\text{O}_2/(\text{mg}$ of $\text{Chl}\cdot\text{h}$). The PSII samples (PSII from spinach at 3.2 mg of Chl/mL and PSII from *S. elongatus* at 0.8 mg of Chl/mL) were loaded into quartz EPR tubes and dark-adapted for 1 h at 0 °C. The samples were synchronized in the S_1 state by one preflash (38). After a dark period of 10 min at room temperature, 1 mM phenyl-*p*-benzoquinone dissolved in either methanol or ethanol was added (the final concentration of alcohol was 3%). After illumination by the indicated number of flashes, the samples were frozen in the dark to 200 K (ethanol, solid CO_2), then degassed at 200 K as already described (25), and then transferred to 77 K.

Flash illumination at room temperature was provided by a Nd–YAG laser (532 nm, 550 mJ, 8 ns) Spectra Physics GCR-230-10. Near-IR illumination of the samples was done in a nitrogen gas flow system (Bruker, B-VT-1000) and was provided by a laser diode emitting at 820 nm (Coherent, diode S-81-1000C) with a power of 600–700 mW at the level of the sample. CW-EPR spectra were recorded at liquid helium temperatures as previously described (24, 25) with a Bruker ESP300 X-band spectrometer equipped with an Oxford Instruments cryostat.

RESULTS

Figure 1 shows the CW-EPR spectra recorded on PSII isolated either from spinach (panel A) or from *S. elongatus* (panel B) after illumination by the indicated number of flashes in the presence of methanol. After the first flash, the S_2 multiline signal is observed in both samples. This signal decreased after the second flash and a multiline signal different from that detected after the first flash is observed after the third and fourth flash. After the third flash (although there is a contribution from the S_2 multiline signal), the S_0 state is the predominant S state and therefore the multiline signal recorded in these conditions very likely originates from the S_0 state in both samples. The oscillating pattern was simulated from the amplitudes of both the S_2 and S_0 signals. The fits were calculated by using (a) the S_2 multiline signal recorded after the first, the second, and the fifth flash and (b) the S_0 multiline signal recorded after the third and fourth flash. In both experiments the misses were found to be $\approx 11\% \pm 2\%$ and the starting S -state distribution was $\approx 8\% \pm 2\%$ S_0 and $\approx 92\% \pm 2\%$ S_1 (not shown but see ref 39).²

Spectra in panel B of Figure 1 exhibit the characteristic Mn^{II} hexaquo EPR signal with six lines spaced by ≈ 90 G between 3100 and 3700 G. Amplitude of this signal varies from batch to batch and may be very small, as in samples used in Figures 3 and 4 (see below). Detection of this signal

² A careful examination of the 0 flash spectra in Figure 1 shows that the very small multiline signals present in these samples originate from a low proportion of centers in the S_0 state. Indeed, these spectra are similar to the multiline signals that are detected in the fourth flash samples and that can be considered as essentially pure S_0 multiline signal.

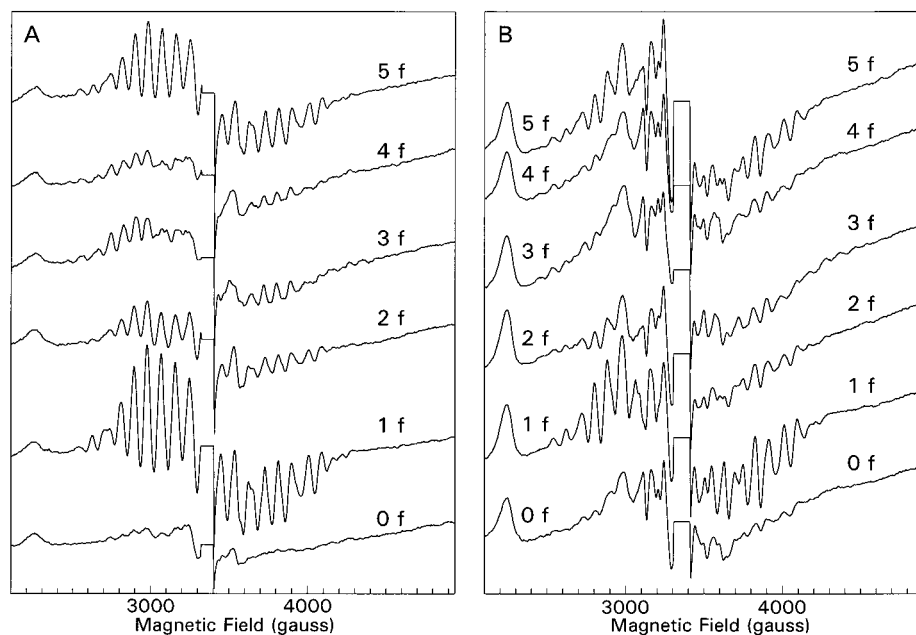


FIGURE 1: CW-EPR spectra recorded on PSII isolated either from spinach (panel A) or from *S. elongatus* (panel B) after a series of saturating laser flashes (1 Hz) in the presence of methanol. Instrument settings: modulation amplitude, 25 G; microwave power, 20 mW; microwave frequency, 9.4 GHz; modulation frequency, 100 kHz. Temperature was 7 K. The central part of the spectra corresponding to the Tyr_D region was deleted.

can normally be prevented by the addition of EDTA. Nevertheless, the presence of high concentrations of Ca²⁺ (i.e. 20–50 mM) in the samples makes the addition of EDTA ineffective. Spectra in panel B (Figure 1) also exhibit intense features at ≈ 2230 and ≈ 3030 G, which are the g_z and g_y resonances, respectively, arising from the oxidized form of a low-spin cytochrome heme. These features are much more intense in *S. elongatus* than in plant PSII. As proposed previously (25), it seems likely that the increase in these signals arises from cyt *c*₅₅₀, which is known to be associated with PSII in cyanobacteria (40–44) and is present in this preparation (37).

The amplitude of the g_z and g_y resonances of the cytochrome signal, which is recorded with a saturating microwave power in panel B of Figure 1, varies significantly with the flash number. Such variations are not observed with the g_z and g_y resonances of cyt *b*₅₅₉ (see panel A in Figure 1, for example). Such an effect could arise from a change in the magnetic relaxation properties of cyt *c*₅₅₀ caused by changes in the redox state and hence the magnetic state of the Mn₄ cluster, just as observed for Tyr_D (38). This possibility was tested by the experiment reported in Figure 2.

In Figure 2, the cytochrome g_z signal was recorded after zero (spectra a), one (spectra b), and three (spectra c) flashes under nonsaturating (panel A) and saturating (panel B) conditions. As a control, panels C and D in Figure 2 also show the Tyr_D signal recorded, respectively, under nonsaturating and saturating conditions. In saturating conditions, formation of the S₂ and S₀ states results in the well-known saturation enhancement effect on Tyr_D (38). Panel A shows that by use of nonsaturating conditions, the amplitude of the heme g_z signal was unchanged after one and three flashes. This indicates that no change in the redox state of the cytochrome occurred. In contrast, under saturating conditions (panel B), the amplitude of the g_z signal of the heme was larger after the first and third flash. Therefore, as for Tyr_D, formation of the S₂ and S₀ states induces a saturation

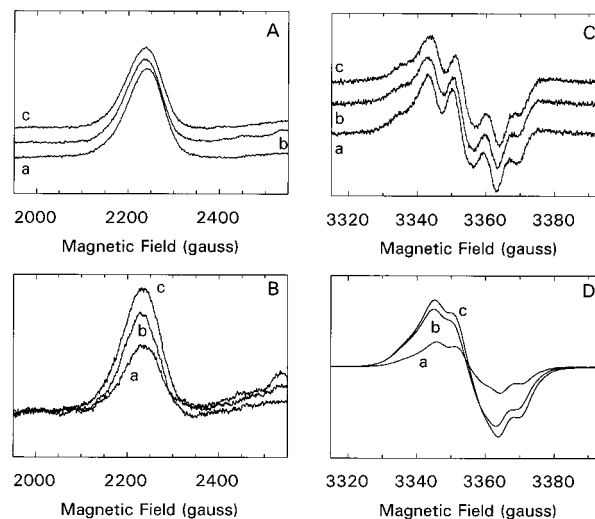


FIGURE 2: (Panels A and B) g_z heme spectra recorded after zero (spectra a), one (spectra b), and three flashes (spectra c). Instrument settings: modulation amplitude, 32 G; frequency, 9.4 GHz; modulation frequency, 100 kHz; microwave power, 20 mW. Temperature was 15 K in panel A and 7 K in panel B. (Panels C and D) Tyr_D spectra recorded at 7 K after zero (spectra a), one (spectra b), and three flashes (spectra c). Instrument settings: modulation amplitude, 2.8 G; microwave power, 0.5 μ W for panel C and 5 mW for panel D; microwave frequency, 9.4 GHz; modulation frequency, 100 kHz.

enhancement effect on the relaxation rate of the heme. Since this relaxation effect is not seen for the heme of cyt *b*₅₅₉, these results can be taken as a further indication that the heme signal in *S. elongatus* arises mainly from cyt *c*₅₅₀.³

³ The microwave power saturation curve of the g_z signal measured at 7 K can be fitted with the inhomogeneity parameter $b \approx 1.5$ and the microwave power at half saturation $P_{1/2} \approx 1.5$ mW in the zero-flash sample and $P_{1/2} \approx 2.4$ mW in the one-flash sample. When plotted with the same vertical scale, spectrum a in Figure 2B appears 3.3 times smaller than spectrum a in Figure 2A. This explains the apparent lower signal-to-noise ratio in panel B than in panel A of Figure 2.

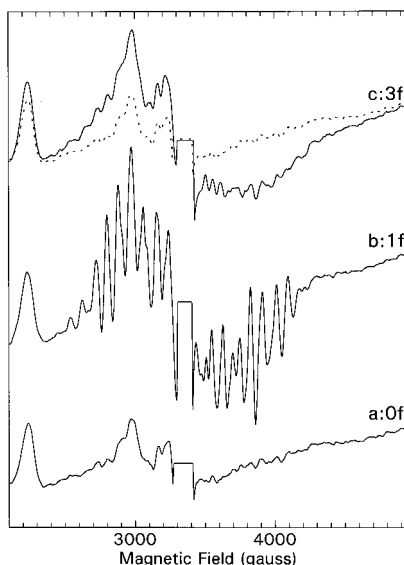


FIGURE 3: CW-EPR spectra after a series of saturating laser flashes (1 Hz) in the presence of ethanol recorded on PSII isolated from *S. elongatus* at 8 K with a microwave power of 20 mW. Spectra a, b, and c were recorded after zero, one, and three flashes, respectively. The dotted line is the 0 flash spectrum. Other instrument settings were as in Figure 1.

Figure 3 shows the EPR spectra recorded at 8 K on PSII from *S. elongatus* in the presence of ethanol. Spectra were recorded in a dark-adapted sample, i.e., in the S_1 state (spectrum a); after one flash, i.e., in the S_2 state (spectrum b); and after three flashes, i.e., in the S_0 state (spectrum c). After the first flash, the S_2 multiline signal is observed (Figure 3b). After the third flash, a different signal is clearly observed (Figure 3c) when compared to the zero flash spectrum (dotted line). The S_0 signal recorded is slightly distorted due to the change in the saturation properties of a heme signal attributed to cyt c_{550} (see above).

Previous results have shown that in plant PSII the methanol-induced S_0 signal was still detectable at 4.2 K (26–29), in contrast with the S_2 multiline signal, which is totally saturated at 4.2 K at a microwave power of 40 mW. Figure 4A shows the EPR spectra recorded at 4.2 K on PSII from *S. elongatus* in the presence of ethanol. Spectra were recorded in a dark-adapted sample i.e., in the S_1 state (spectrum a); after one flash, i.e., in the S_2 state (spectrum b); and after three flashes, i.e., in the S_0 state (spectrum c). Spectrum c shows that the S_0 signal in *S. elongatus*, with ethanol instead of methanol, exhibits a similar power dependence in that it is easily detectable at 4.2 K. At this temperature, the cyt c_{550} and S_2 multiline signals were so saturated that they did not contribute significantly to the spectra (see spectra a and b in Figure 4A). Also shown in Figure 4B is the comparison between the S_0 signals in *S. elongatus* obtained at 4.2 K by subtracting the zero-flash spectrum from the three-flash spectrum with either ethanol (spectrum d) or methanol (spectrum e).

Figure 5 shows the light-minus-dark difference spectra recorded at 7–8 K under the different conditions reported here. In addition, in the S_0 states (spectra a, b, and c), the residual S_2 multiline signal present after the third flash (≈ 5 –8% of that detected after the first flash) has also been removed by interactive subtraction.⁴ Amplitude of the S_2 multiline signal after the third flash determined by interactive

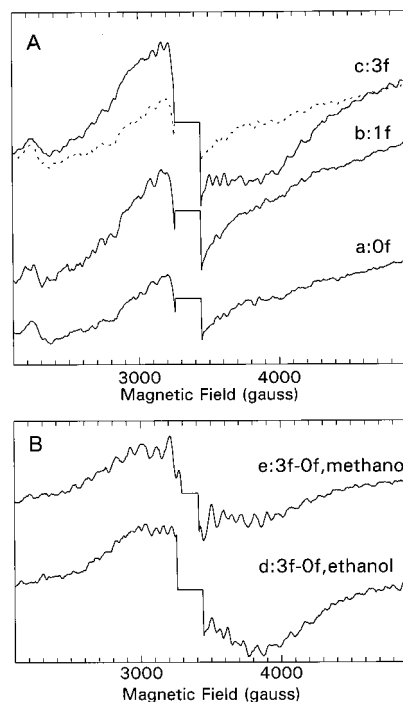


FIGURE 4: (Panel A) CW-EPR spectra after a series of saturating laser flashes (1 Hz) in the presence of ethanol recorded on PSII isolated from *S. elongatus* at 4.2 K with a microwave power of 20 mW. Spectra a, b, and c were recorded after zero, one, and three flashes, respectively. The dotted lines is the zero-flash spectrum. Other instrument settings were as in Figure 1. (Panel B) Spectrum d corresponds to spectrum c minus spectrum a from panel A. Spectrum e corresponds to the three-flash spectrum minus the zero-flash spectrum recorded at 4.2 K in sample with methanol present. The central part of the spectra corresponding to the Tyr_D region was deleted.

subtraction (i.e., 5–8%; see above) is close to that expected from the fit of the oscillating pattern (i.e., 6.2%). A similar procedure has been already used to obtain a pure S_0 signal (28). Spectrum b (Figure 5) corresponds to the S_0 state formed in the presence of methanol in *S. elongatus*. This S_0 multiline signal differs from that in plants (spectrum a) in that the hyperfine structure is less resolved between 2400 and 3400 G and more resolved between 3400 and 4500 G.

In the presence of ethanol, the S_0 multiline signal in *S. elongatus* also consists of a very broad S-shaped signal with rather poorly resolved hyperfine lines (Figure 5, spectrum c). The magnetic field positions of these lines are different from those observed in spectra a and b and also different from those observed in the S_2 multiline signal. Moreover, the S_0 signals measured at 4.2 K (Figure 4), that is under conditions where the S_2 multiline signal is not detected, exhibits the same hyperfine structure as at 8 K. This makes it unlikely that the hyperfine structures present in the S_0 signals in Figure 5 arise from a small proportion of residual S_2 multiline signal. Moreover, double integration of spectra b and c shows that the S_0 signal recorded in the presence of ethanol has an amplitude similar to that recorded in the presence of methanol (not shown).

⁴ Interactive subtraction is a standard computer-assisted spectrum manipulation in which an unknown spectral component (b) can be extracted from a mixture (y) of two spectra by subtracting a proportion of a second known spectral component (x). The proportion (a) of the known spectral component in the mixture is gradually varied until the difference spectrum ($y - ax$) is considered to contain no contribution from the known spectrum.

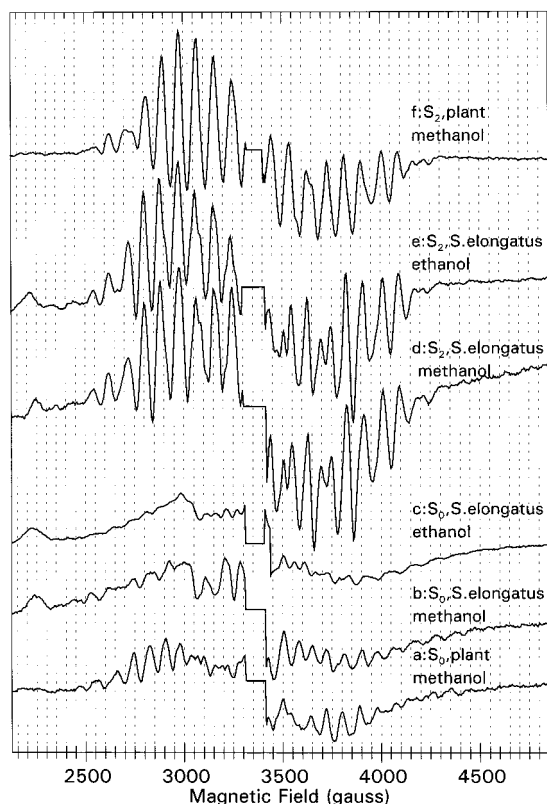


FIGURE 5: Light-minus-dark CW-EPR spectra obtained from spectra shown in Figures 1 and 3 by subtracting the zero-flash sample. For spectra a, b, and c the residual S_2 multilines signal present after three flashes was also subtracted. Spectra a and f are approximately scaled to other spectra by using the Tyr_D signal as a reaction center concentration standard.

Spectra d and e in Figure 5 shows the S_2 multilines signals that were obtained in *S. elongatus* in the presence of methanol and ethanol, respectively. They appear almost identical. The S_2 signal in PSII from plants in the presence of ethanol is also very similar, if not identical, to spectra d and e (not shown). In contrast, methanol addition to plant PSII results in a completely different S_2 multilines signal (spectrum f).

Figures 3 and 5 show that the S_2 multilines signal recorded in *S. elongatus* in the presence of methanol is similar to that recorded in the presence of ethanol. Furthermore, methanol does not prevent the formation of the high-spin S_2 EPR signals. Figure 6 shows that IR illumination on a one-flash sample with methanol present (spectrum a) induced signals between $g = 5$ and $g = 9$ in about 40–50% of the reaction centers (spectrum b). The IR induced signals (spectrum c) are very similar to those described previously in the absence of methanol (25). Therefore, in *S. elongatus* the situation is different from that in plants, where methanol modifies the S_2 spectrum and renders it insensitive to the IR illumination.

DISCUSSION

The experiments reported above show that the S_0 state in PSII isolated from *S. elongatus* exhibits an EPR multilines signal. In contrast with plant PSII, detection of such a signal does not require the addition of methanol (however, ethanol is used as a solvent for the artificial electron acceptor). With ethanol present, although the width of the signal is similar, the hyperfine lines of the S_0 multilines signal are less resolved than with methanol present. The S_0 multilines signal is

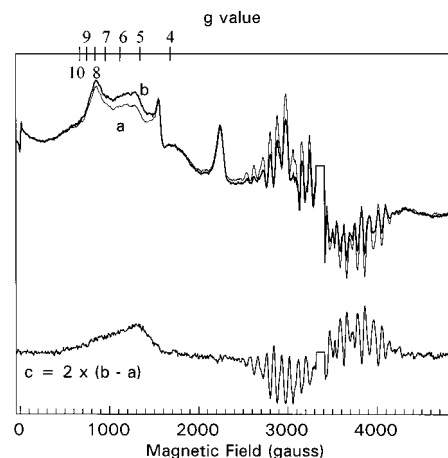


FIGURE 6: Spectrum a was recorded after one flash with methanol present. Spectrum b was recorded after a further 820 nm illumination given at 150 K. Spectrum c shows the spectrum obtained by subtracting the spectrum recorded before the IR illumination from that recorded after the IR illumination. Instrument settings were as in Figure 1.

centered near $g = 2$, it is spread over ≈ 2380 G, and in the presence of methanol it is constituted of 25 resolved lines spaced by 65–95 G. The presence of the $S = 1/2$ signal in the S_0 state even without methanol and the effect of methanol in improving the resolution of the hyperfine lines support the suggestion (26, 27) that a $S = 1/2$ state also exists in plant PSII in the absence of methanol. Earlier we reported preliminary field-swept echo experiments that also appeared to be in agreement with this hypothesis (39); however, further experiments were unable to confirm this observation (not shown). At present, we have found no conditions under which an S_0 signal in plant PSII is detectable without methanol (but see ref 27).

In *S. elongatus*, in contrast to plant PSII, methanol had no effect on the S_2 multilines signal and its susceptibility to IR light. Irrespective of the alcohol added, the S_2 multilines signal in *S. elongatus* is very similar to that detected in plant PSII in the absence of methanol. In plants, two populations of PSII reaction centers have been defined on the basis of behavior of the S_2 state: those centers in which the spin state is changed by IR light and those centers that are insensitive to IR light (45). The total S_2 multilines signal seems to result from the superposition of the two types of multilines signals that originate from these two PSII populations. The S_2 population that is insensitive to IR light gives rise to a “narrow” multilines signal characterized by stronger central lines and weaker outer lines. The IR-susceptible S_2 population gives rise to a “broad” multilines signal in which the intensity of the outer lines, at low and high field, are larger relative to those in the narrow multilines signal (45). The spectral properties of the methanol S_2 multilines signal were found to correspond to PSII centers that are insensitive to IR light, and indeed, the yield of the IR-induced spin conversion in the S_2 state in the presence of methanol was close to zero (39). In the presence of methanol the Mn_4 structure in PSII from plants appears therefore to be more homogeneous as measured by its sensitivity to IR light. From the present observations, it can also be concluded that in *S. elongatus* methanol does not appear to interact with the Mn_4 cluster in the S_2 state.

From ESEEM and electron–nuclear double resonance (ENDOR) experiments it has been proposed that methanol binds to Mn^{III}–Mn^{IV} complexes (47) and to the Mn₄ cluster in the S₂ state (46). From ESEEM experiments done in the S₀ and S₂ states of plant PSII (39), with CD₃OH and CH₃OH, two methanol effects have been found in the S₀ state: (i) a greater access of the Mn₄ cluster to the solvent than in the S₂ state and possibly (ii) a weak specific interaction. The phenomena measured here (the form of the CW-EPR signals and, for S₂, its sensitivity to IR light) could be related to either (or both) types of methanol effects described above (i.e., specific binding or solvent effects). This can be tested by further experiments using pulsed EPR methods. In particular, if the changes in the CW-EPR spectra correspond to methanol binding and/or solvent effects, then we might predict decreased deuterated methanol couplings.

From Figure 5 it appears that the S₀ multiline signal detected in *S. elongatus* differs slightly from that detected in plants. The main difference is the presence of more resolved lines at high field and less resolved lines at low field. This behavior results from slight changes in the magnetic coupling between the manganese ions. Differences in the magnetic couplings between the Mn ions of the Mn₄ cluster of plants and *S. elongatus* have already been observed (25). Indeed, in the S₂ state, the IR-induced signals in the PSII from *S. elongatus* slightly differed from those induced in PSII from plants. The value of the E/D ratio for the IR-induced state found in PSII isolated from *S. elongatus* was found to be more rhombic than that in PSII from plants. This difference would imply, for example, differences in the ligand environment of the Mn₄ cluster.

In the course of this study we observed changes in a low-spin heme EPR signal that indicate a magnetic coupling between the heme and the manganese cluster. Cyt *b*₅₅₉ is present in cyanobacteria but, in plants, it does not show such a magnetic effect. Therefore, the magnetic effect reported above is attributed to the cyt *c*₅₅₀ heme, which binds on the electron donor side of PSII in cyanobacteria and seems to play a role analogous to the 17 and 24 kDa extrinsic polypeptides of plants (40–44). Since the PSII from *S. elongatus* are dimeric, a magnetic interaction between the heme of cyt *c*₅₅₀ of one PSII monomer and the Mn₄ cluster of the neighboring PSII monomer cannot be excluded. The existence of this magnetic interaction could be the basis of future structural studies.

NOTE ADDED IN PROOF

We have recently observed an S₀ signal in *S. elongatus* comparable to that in Figure 4d when ethanol is replaced with DMSO. Thus, an alcohol is not required to observe this signal.

REFERENCES

1. Michel, H., and Deisenhofer, J. (1988) *Biochemistry* 27, 1–7.
2. Britt, R. D. (1996) in *Oxygenic photosynthesis: The light reactions* (Ort, D. R., and Yocum, C. F., Eds.) pp 137–164, Kluwer Academic Publishers, Dordrecht, The Netherlands.
3. Debus, R. J. (1992) *Biochim. Biophys. Acta* 1102, 269–352.
4. Rutherford, A. W. (1989) *Trends Biochem. Sci.* 14, 227–232.
5. Rutherford, A. W., Zimmermann, J.-L., and Boussac, A. (1992) in *The photosystems: Structure, function and molecular biology* (Barber, J., Ed.) Chapter 5, pp 179–229, Elsevier Science Publishers, New York.
6. Yachandra, V. K., Sauer, K., and Klein, M. P. (1996) *Chem. Rev.* 96, 2927–2950.
7. Dismukes, G. C., and Siderer, Y. (1981) *Proc. Natl. Acad. Sci. U.S.A.* 78, 274–278.
8. Brudvig, G. W. (1989) in *Advanced EPR: Applications in Biology and Chemistry* (Hoff, A. J., Ed.) Chapter 24, pp 839–864, Elsevier, Amsterdam, The Netherlands.
9. Dismukes, G. C. (1993) in *Polynuclear manganese enzymes, Bioinorganic catalysis* (Reedijk, J., Ed.) pp 317–346, Marcel Dekker, Inc., New York.
10. Casey, J. L., and Sauer, K. (1984) *Biochim. Biophys. Acta* 767, 21–28.
11. DeRose, V. J., Yachandra, V. K., McDermott, A. E., Britt, R. D., Sauer, K., and Klein, M. P. (1991) *Biochemistry* 30, 1335–1341.
12. McDermott, A. E., Yachandra, V. K., Guiles, R. D., Cole, J. L., Dexheimer, S. L., Britt, R. D., Sauer, K., and Klein, M. P. (1988) *Biochemistry* 27, 4021–4031.
13. Kirilovsky, D. L., Boussac, A. G. P., van Mieghem, F. J. E., Ducruet, J.-M. R. C., Sétif, P. R., Yu, J., Vermaas, W. F. J., and Rutherford, A. W. (1992) *Biochemistry* 31, 2099–2107.
14. Tang, X.-S., and Diner, B. A. (1994) *Biochemistry* 33, 4594–4603.
15. Noren, G. H., Bøerner R. J., and Barry, B. A. (1991) *Biochemistry* 30, 3943–3950.
16. Rutherford, A. W., Seibert, M., and Metz, J. G. (1988) *Biochim. Biophys. Acta* 932, 171–176.
17. Schiller, H., Klingelhöfer, S., Dörner, W., Senger, H., and Dau, H. (1995) in *Photosynthesis: From Light to Biosphere* (Mathis, P., Ed.) Vol. II, pp 463–466, Kluwer Academic Publishers, Dordrecht, The Netherlands.
18. Zimmermann, J.-L., and Rutherford, A. W. (1986) *Biochemistry* 25, 4609–4615.
19. van Vliet, P. (1996) Thesis, Landbouwniversiteit Wageningen.
20. van Vliet, P., and Rutherford, A. W. (1996) *Biochemistry* 35, 1829–1839.
21. Lindberg, K., and Andréasson, L.-E. (1996) *Biochemistry* 35, 14259–14267.
22. Boussac, A., Girerd, J.-J., and Rutherford, A. W. (1996) *Biochemistry* 35, 6984–6989.
23. Horner, O., Rivière, E., Blondin, G., Un, S., Rutherford, A. W., Girerd, J.-J., and Boussac, A. (1998) *J. Am. Chem. Soc.* 120, 7924–7928.
24. Boussac, A., Un, S., Horner, O., and Rutherford, A. W. (1998) *Biochemistry* 37, 4001–4007.
25. Boussac, A., Kuhl, H., Un, S., Rögner, M., and Rutherford, A. W. (1998) *Biochemistry* 37, 8995–9000.
26. Messinger, J., Nugent, J. H. A., and Evans, M. C. W. (1997) *Biochemistry* 36, 11055–11060.
27. Messinger, J., Robblee, J. H., Yu, W. O., Sauer, K., Yachandra, V. K., and Klein, M. P. (1997) *J. Am. Chem. Soc.* 119, 11349–11350.
28. Åhring, K. A., Peterson, S., and Styring, S. (1997) *Biochemistry* 36, 13148–13152.
29. Åhring, K. A., Peterson, S., and Styring, S. (1998) *Biochemistry* 37, 8115–8120.
30. da Fonseca, P., Maghlaoui, K., Hankamer, B., Büchel, C., and Barber, J. (1998) in *Photosynthesis: Mechanism and Effects* (Garab, G., Ed.) Vol. II, pp 969–972, Kluwer Academic Publishers, Dordrecht, The Netherlands.
31. Zouni, A., Lüneberg, C., Fromme, P., Schubert, W. D., Saenger, W., and Witt, H. T. (1998) in *Photosynthesis: Mechanism and Effects* (Garab, G., Ed.) Vol. II, pp 925–928, Kluwer Academic Publishers, Dordrecht, The Netherlands.
32. Govindjee, Koike, H., and Inoue, Y. (1985) *Photochem. Photobiol.* 42, 579–585.
33. Koike, H., Hanssum, B., Inoue, Y., and Renger, G. (1987) *Biochim. Biophys. Acta* 893, 524–533.
34. Tramontini, L. S., McColl, S., and Evans, E. H. (1996) *Photosynth. Res.* 50, 233–241.
35. Pauli, S., Schlodder, E., and Witt, H. T. (1992) *Biochim. Biophys. Acta* 1099, 203–210.

36. Rögner, M., Nixon, P. J., and Diner, B. A. (1990) *J. Biol. Chem.* 265, 6189–6196.
37. Kuhl, H., Krieger, A., Seidler, A., Boussac, A., Rutherford, A. W., and Rögner, M. (1998) in *Photosynthesis: Mechanism and Effects* (Garab, G., Ed.) Vol. II, pp 1001–1004, Kluwer Academic Publishers, Dordrecht, The Netherlands.
38. Styring, S., and Rutherford, A. W. (1988) *Biochemistry* 27, 4915–4923.
39. Boussac, A., Deligiannakis, Y., and Rutherford, A. W. (1998) in *Photosynthesis: Mechanism and Effects* (Garab, G., Ed.) Vol. II, pp 1233–1240, Kluwer Academic Publishers, Dordrecht, The Netherlands.
40. Shen, J.-R., Ikeuchi, M., and Inoue, Y. (1992) *FEBS Lett.* 301, 145–149.
41. Shen, J.-R., and Inoue, Y. (1993) *J. Biol. Chem.* 268, 20408–20413.
42. Nishiyama, Y., Hayashi, H., Watanabe, T., and Murata, N. (1994) *Plant Physiol.* 105, 1313–1319.
43. Navarro, J. A., Hervás, M., De la Cerda, B., and De la Rosa, M. (1995) *Arch. Biochem. Biophys.* 318, 46–52.
44. Shen, J.-R., Burnap, R. L., and Inoue, Y. (1995) in *Photosynthesis: from light to biosphere* (Mathis, P., Ed.) Vol. II, pp 559–562, Kluwer Academic Publishers, Dordrecht, The Netherlands.
45. Boussac, A. (1997) *J. Biol. Inorg. Chem.* 2, 580–585.
46. Force, D. A., Randall, D. W., Lorigan, G. A., Clemens, K. L., and Britt, R. D. (1998) *J. Am. Chem. Soc.* 120, 13321–13333.
47. Randall, D. W., Gelasco, A., Caudle, M. T., Pecoraro, V. L., and Britt, R. D. (1997) *J. Am. Chem. Soc.* 119, 4481–4491.

BI990845R